Ab initio calculations of the atomic and electronic structure of $CaTiO_3$ (001) and (011) surfaces

R. I. Eglitis and David Vanderbilt
Department of Physics and Astronomy, Rutgers University,
136 Frelinghuysen Road, Piscataway, New Jersey 08854-8019, USA
(Dated: July 30, 2008)

We present the results of calculations of surface relaxations, energetics, and bonding properties for $CaTiO_3$ (001) and (011) surfaces using a hybrid B3PW description of exchange and correlation. We consider both CaO and TiO_2 terminations of the non-polar (001) surface, and Ca, TiO and O terminations of the polar (011) surface. On the (001) surfaces, we find that all upper-layer atoms relax inwards on the CaO-terminated surface, while outward relaxations of all atoms in the second layer are found for both terminations. For the TiO_2-terminated (001) surface, the largest relaxations are on the second-layer atoms. The surface rumpling is much larger for the CaO-terminated than for the TiO_2-terminated (001) surface, but their surface energies are quite similar at 0.94 eV and 1.13 eV respectively. In contrast, different terminations of the (011) $CaTiO_3$ surface lead to very different surface energies of 1.86 eV, 1.91 eV, and 3.13 eV for the O-terminated, Ca-terminated, and TiO-terminated (011) surface respectively. Our results for surface energies contrast sharply with those of Zhang *et al.* [Phys. Rev. B **76**, 115426 (2007)], where the authors found a rather different pattern of surface energies. We predict a considerable increase of the Ti-O chemical bond covalency near the (011) surface as compared both to the bulk and to the (001) surface.

PACS numbers: 68.35.Ct, 68.35.Md, 68.47.Gh

I. INTRODUCTION

Oxide perovskites are in demand for a variety of industrial applications as a result of their diverse physical properties.[1,2,3] For example, $CaTiO_3$ is a cubic perovskite that is widely used in electronic ceramic materials and as a key component of synthetic rock to immobilize high-level radioactive waste.[4] Thin films of ABO_3 perovskite ferroelectrics are important for many applications.[1,4] In particular, the titanates are interesting materials regarding their electrochemical properties and are promising as components for electrodes and sensors. Surface properties of $CaTiO_3$ are important for catalysis and for epitaxial growth of high T_c superconductors. For all these applications, the surface structure and the associated surface electronic and chemical properties are of primary importance.

In view of this technological importance, it is surprising that there have been so few *ab initio* studies of $CaTiO_3$ surface atomic and electronic structure. For the $CaTiO_3$ (001) surface we are only aware of the work of Wang *et al.*[5] and Zhang *et al.*[6] In contrast, several other ABO_3 perovskite (001) surfaces have been widely studied. For example, *ab initio*[7,8,9,10,11,12,13,14,15,16,17,18,19,20,21] and classical shell-model[22,23] studies were published for the (001) surfaces of $SrTiO_3$. The (001) surfaces of cubic perovskites have also been extensively investigated experimentally. For example, the $SrTiO_3$ (001) surface relaxations and rumplings have been studied by means of low energy electron diffraction (LEED), reflection high-energy electron diffraction (RHEED), medium energy ion scattering (MEIS), and surface x-ray diffraction (SXRD) measurements.[24,25,26,27,28] The status of the degree of agreement between theory and experiment for these $SrTiO_3$ surfaces is summarized in Ref. [7].

ABO_3 perovskite (011) surfaces are considerably less-well studied than (001) surfaces, both experimentally and theoretically. However, there has been a surge of recent interest, focusing mainly on $SrTiO_3$, in which STM, UPS, XPS,[33,34] and Auger spectroscopies as well as LEED studies[35,36,37,38,39] have been carried out. On the theory side, the first *ab initio* calculations for $SrTiO_3$ (011) surfaces were performed by Bottin *et al.*,[29] who carried out a systematic study of the electronic and atomic structures of several (1×1) terminations of the (011) polar orientation of the $SrTiO_3$ surface. They found that the electronic structure of the stoichiometric SrTiO and O_2 terminations showed marked differences with respect to the bulk as a consequence of the polarity compensation. Later, Heifets *et al.*[30] performed *ab initio* Hartree-Fock (HF) calculations for four possible non-polar terminations (TiO, Sr, and two kinds O terminations) of the $SrTiO_3$ (011) surface. The authors found that the surface energy of the O-terminated (011) surface is close to that of the (001) surface, suggesting that both (011) and (001) surfaces can coexist in polycrystalline $SrTiO_3$. Most recently, we performed an *ab initio* study of $SrTiO_3$ (011) surfaces[7] using a hybrid Hartree-Fock (HF) and density-functional theory (DFT) exchange-correlation functional, in which HF exchange is mixed with Becke's three-parameter DFT exchange and combined with the nonlocal correlation functional of Perdew and Wang (B3PW).[40,41] Our calculations indicated a remarkably large increase in the Ti-O bond covalency at the TiO-terminated (011) surface, significantly larger than for the (001) surfaces.

Regarding other ABO_3 (011) surfaces, Heifets *et al.*[31] investigated the atomic structure and charge redistribu-

tion of different terminations of $BaZrO_3$ (011) surfaces using density-functional methods. They found that the O-terminated (011) surface had the smallest cleavage energy among (011) surfaces, but that this value was still twice as large as the cleavage energy needed for the formation of a pair of complementary (001) surfaces. Moreover, we recently performed *ab initio* B3PW calculations for the technologically important $BaTiO_3$ and $PbTiO_3$ (011) surfaces.[32] Our calculated surface energies showed that the TiO_2-terminated (001) surface is slightly more stable than the BaO- or PbO-terminated (001) surface for both materials, and that O-terminated $BaTiO_3$ and TiO-terminated $PbTiO_3$ (011) surfaces have surface energies close to that of the (001) surface.

The only existing *ab initio* study of $CaTiO_3$ (011) polar surfaces was performed by Zhang *et al.*[6] In addition to the (001) surfaces, they studied four possible non-polar terminations of the (011) surface, namely the TiO, Ca, asymmetric A-type O, and symmetric B-type O terminations. The results indicated that the most favorable surfaces are the CaO-terminated (001) surface, the A-type O-terminated (011) surface, and the TiO_2-terminated (001) surface, in that order.

With the sole exception of the calculation on $CaTiO_3$ by Zhang *et al.*,[6] all of the first-principles and shell-model studies of ABO_3 perovskite surface energies[7,12,16,23,30,32,42] have found that the lowest-energy (001) surface is lower in energy than any of the (011) terminations. Zhang *et al.*,[6] on the contrary, reported a surface energy of 0.837 eV for their "A-type" O-terminated (011) surface of $CaTiO_3$, to be compared with 1.021 eV for the TiO_2-terminated (001) surface. Because this result contrasts sharply with the other previous calculations, we were particularly motivated to check this result independently in our current study.

In this study, we have performed predictive *ab initio* calculations for $CaTiO_3$ (001) and (011) surfaces, using the same B3PW approach as in our previous work.[7,32] As in the work of Zhang *et al.*,[6] we do not explicitly include octahedral rotations in the surface calculations, even though such rotations are likely to be more important for $CaTiO_3$ than for many other perovskites; we discuss and justify this approximation at the end of Sec. II. In contradiction to the work of Zhang *et al.*,[6] we find that the pattern of surface energies of $CaTiO_3$ is similar to that of other perovskites. In particular, we find that the O-terminated $CaTiO_3$ (011) surface is *higher* in energy than either of the TiO_2- or CaO-terminated (001) surfaces. We also report the surface relaxations and rumplings and the charge redistributions and changes in bond strength that occur at the surface.

The manuscript is organized as follows. In Sec. II we present our computational method and provide details of the surface slab models on which the calculations were performed. The results of our calculations for surface structures, energies, charge distributions, and bond populations are reported in Sec. III. Finally, we discuss the results and present our conclusions in Sec. IV.

II. COMPUTATIONAL METHOD AND SURFACE SLAB CONSTRUCTION

To perform the first-principles DFT-B3PW calculations we used the CRYSTAL-2003 computer code,[43] which employs Gaussian-type functions (GTFs) localized at atoms as the basis for an expansion of the crystalline orbitals. The features of the CRYSTAL-2003 code that are most important for this study are its ability to calculate the electronic structure of materials within both Hartree-Fock and Kohn-Sham Hamiltonians and its ability to treat isolated 2D slabs without artificial repetition along the z-axis. However, in order to employ the linear combination of atomic orbitals (LCAO)-GTF method, it is desirable to have optimized basis sets (BS). The BS optimization for $SrTiO_3$, $BaTiO_3$, and $PbTiO_3$ perovskites was developed and discussed in Ref. [44]. Here we employ this BS, which differs from that used in Refs. [12,13] by inclusion of polarizable d-orbitals on O ions. It was shown[44] that this leads to better agreement of the calculated lattice constant and bulk modulus with experimental data. For the Ca atom we used the same BS as in Ref. [45].

Our calculations were performed using the hybrid exchange-correlation B3PW functional involving a hybrid of non-local Fock exact exchange, LDA exchange and Becke's gradient corrected exchange functional,[40] combined with the nonlocal gradient corrected correlation potential by Perdew and Wang.[41] The Hay-Wadt small-core effective core pseudopotentials (ECP) were adopted for Ca and Ti atoms.[46] The small-core ECP's replace only the inner core orbitals, while orbitals for sub-valence electrons as well as for valence electrons are calculated self-consistently. Oxygen atoms were treated with the all-electron BS.

The reciprocal space integration was performed by sampling the Brillouin zone of the five-atom cubic unit cell with an 8×8×8 Pack-Monkhorst grid for the bulk,[47] and an 8×8 grid for the slab structure, providing a balanced summation in direct and reciprocal spaces. To achieve high accuracy, large enough tolerances of 7, 8, 7, 7, and 14 were chosen for the Coulomb overlap, Coulomb penetration, exchange overlap, first exchange pseudo-overlap, and second exchange pseudo-overlap parameters, respectively.[43]

The $CaTiO_3$ (001) surfaces were modeled with two-dimensional slabs consisting of several planes perpendicular to the [001] crystal direction. To simulate $CaTiO_3$ (001) surfaces, we used slabs consisting of seven alternating TiO_2 and CaO layers, with mirror symmetry preserved relative to the central layer. The 17-atom slab with CaO-terminated surfaces and the 18-atom slab with TiO_2-terminated surfaces are shown in Figs. 1(a) and (b) respectively. These slabs are non-stoichiometric, with unit-cell formulae $Ca_4Ti_3O_{10}$ and $Ca_3Ti_4O_{11}$, respectively. These two (CaO and TiO_2) terminations are the only possible flat and dense (001) surface terminations of the perovskite structure. The sequence of layers with

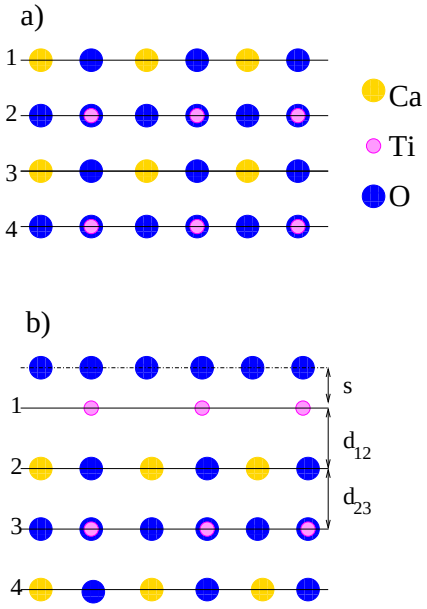

FIG. 1: (Color online.) Side view of $CaTiO_3$ (001) surfaces. (a) CaO-terminated surface. (b) TiO_2-terminated surface, with definitions of surface rumpling s and the near-surface interplanar separations Δd_{12} and Δd_{23}.

(001) orientation, and the definitions of the surface rumpling s and the interplane distances Δd_{12} and Δd_{23}, are illustrated in Fig. 1.

The problem in modeling the $CaTiO_3$ (011) polar surface is that, unlike the $CaTiO_3$ (001) neutral surface, it consists of charged O-O and CaTiO planes, as illustrated in Fig. 2. Assuming nominal ionic charges of O^{2-}, Ti^{4+}, and Ca^{2+}, a simple cleavage would create a negatively-charged O-O surface and a positively-charged CaTiO surface, leading either to an infinite macroscopic dipole moment perpendicular to the surface for a stoichiometric slab terminated by planes of different kinds (O_2 and CaTiO) as in Fig. 3(a), or to a net infinite charge for a non-stoichiometric symmetric slab as shown in Figs. 3(b) and (c). It is known that such crystal terminations make the surface unstable.[48,49] In proper first-principles calculations on slabs of finite thickness, charge redistributions

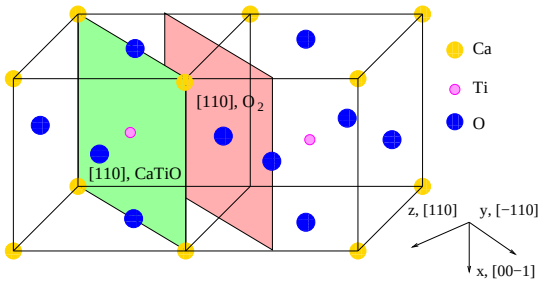

FIG. 2: (Color online.) Sketch of the cubic $CaTiO_3$ perovskite structure showing two (011) cleavage planes that give rise to charged CaTiO and O_2 (011) surfaces.

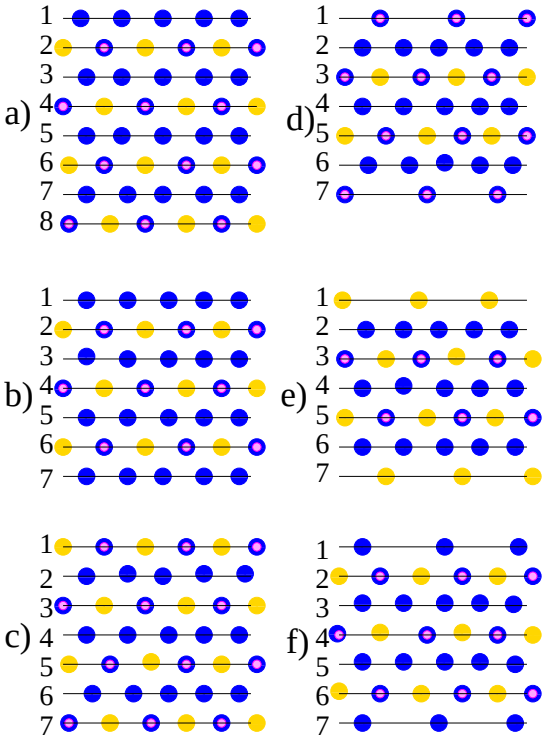

FIG. 3: (Color online.) Possible (011) surface slab models considered in the text. [(a)-(c)] Slabs obtained by simple cleavage, yielding mixed, O-terminated, and CaTiO-terminated polar surfaces, respectively. [(d)-(f)] Slabs with nonpolar TiO-terminated, Ca-terminated, and O-terminated surfaces, respectively.

near the surface arising during the self-consistent field procedure could, in principle, compensate at least partially for these effects. However, previous careful studies for $SrTiO_3$[29,48,50] have demonstrated that the resulting surfaces have a high energy, and that the introduction of surface vacancies provides an energetically less expensive mechanism for compensating the surfaces.

For these reasons, we limit ourselves here to non-polar $CaTiO_3$ (011) surfaces that have been constructed by modifying the composition of the surface layer. Removing the Ca atom from the upper and lower layers of the 7-layer symmetric CaTiO-terminated slab generates a neutral and symmetric 16-atom supercell with TiO-terminated surfaces as illustrated in Fig. 3(d). Removing both the Ti and O atoms from the upper and lower layers of the 7-layer symmetric CaTiO-terminated slab yields a neutral and symmetric 14-atom supercell with Ca-terminated surfaces as shown in Fig. 3(e). Finally, removing the O atom from the upper and lower layers of the 7-layer symmetric O-O terminated slab, we obtain the neutral and symmetric 15-atom supercell with O-terminated surfaces shown in Fig. 3(f). The stoichiometry of these surface terminations, and the number of bonds cleaved, are comprehensively discussed for the case of $SrTiO_3$ in Ref. [29].

Before leaving this Section, it is worth discussing the

TABLE I: Calculated effective charges Q and bond populations P (in e) for bulk $CaTiO_3$.

Ion or bond	Property	Value
Ca	Q	1.782
O	Q	−1.371
Ti	Q	2.330
Ca–O	P	0.006
Ti–O	P	0.084
O–O	P	−0.010

TABLE II: Computed atomic relaxation (in percent of the bulk lattice constant a_0) for the TiO_2- and CaO-terminated $CaTiO_3$ (001) surfaces. Positive values indicate outward displacements.

	CaO-terminated		TiO_2-terminated	
Layer	Ion	This study	Ion	This study
1	Ca	−8.31	Ti	−1.71
	O	−0.42	O	−0.10
2	Ti	1.12	Ca	2.75
	O	0.01	O	1.05

issue of the tilting of TiO_6 octahedra in $CaTiO_3$. Xray and neutron diffraction studies have not definitively established the phase-transition sequence at higher temperature, but clearly show that the crystal adopts an orthorhombic structure with space group P_{bnm} below $\sim$1380 K.[51,52,53,54] This room-temperature ground state has a 20-atom unit cell and is a slight modification from the ideal perovskite structure involving a pattern of tilts of the TiO_6 octahedra according to the $a^-a^-c^+$ pattern in Glazer's notation.[55] The octahedral tilts have also been studied using first-principles calculations.[56,57] Because these tilts are substantial ($\sim$10°),[54] it is possible that they may have some impact on the surface structure and energetics. However, we have not included octahedral tilts in the work presented here for several reasons. First, we want to compare with previous calculations, which have universally not included octahedral tilts. Second, the CRYSTAL-2003 code package does not provide for efficient structural optimization as would be needed to study these tilts, and the larger surface unit cells that would be required would make the calculations impractical. But finally and most importantly, we estimate that the energy scale of the tilts ($\sim$0.1 eV) is small compared to the energy scale of the surface cleavage and relaxation energies (a few eV), so that it is reasonable to neglect them in a first study. The interactions between bulk tilts and surface relaxations remains an interesting question for future study.

III. RESULTS OF CALCULATIONS

A. $CaTiO_3$ bulk atomic and electronic structure

As a starting point of our calculations, we calculated the $CaTiO_3$ bulk lattice constant and found it to be 3.851 Å, slightly smaller than the experimental value of 3.895 Å.[54,58] We used the theoretical bulk lattice constant in the following surface structure calculations. To characterize the chemical bonding and covalency effects, we used a standard Mulliken population analysis for the effective atomic charges Q, bond populations P, and other local properties of the electronic structure as described in, e.g., Refs. [59,60]. Our calculated effective charges and bond populations for bulk $CaTiO_3$ are presented in Table I. The bond population of the Ti–O bond is clearly much larger than that of the Ca–O bond, consistent with partial Ti–O covalency, and the small but negative O–O population indicates a repulsive overlap of oxygen shells in bulk $CaTiO_3$.

B. $CaTiO_3$ (001) surface structure

The atomic displacements obtained using the *ab initio* B3PW method for TiO_2- and CaO-terminated $CaTiO_3$ (001) surfaces are shown in Table II. According to the results of our calculations, atoms of the first surface layer relax inwards, i.e. towards the bulk, for both TiO_2 and CaO-terminated (001) surfaces. The latter result is in disagreement with the previous calculations of Wang *et al.*,[5] who calculated that the first-layer oxygen atoms on the (001) surface should relax outwards by 0.7% of the bulk lattice constant a_0. According to our calculations, they move inwards by 0.42% of a_0. Our calculated inward relaxation of the first-layer oxygen atoms on the CaO-terminated $CaTiO_3$ (001) surface is in line with previous *ab initio* studies dealing with $BaTiO_3$, $PbTiO_3$, and $BaZrO_3$ (001) surfaces,[32,42,61,62] but contrasts with the outward relaxation of first-layer oxygen atoms on the SrO-terminated $SrTiO_3$ (001) surface.[7,20,21] According to the results of our current calculations, outward relaxations are found for all atoms in the second layer for both CaO and TiO_2 terminations of the $CaTiO_3$ (001) surface.

Table II shows that the relaxations of the surface metal atoms are much larger than those of the oxygens on both the TiO_2- and CaO-terminated $CaTiO_3$ (001) surfaces, leading to a considerable rumpling of the outermost surface plane. For the TiO_2-terminated case, we found much larger displacements in the second layer than in the first layer. This behavior contrasts with the atomic relaxation pattern of the TiO_2-terminated $BaTiO_3$ (001) surface, where the upper-layer Ti relaxation is generally larger than the second-layer Ba relaxation.[32,61] However, it is in line with the only existing *ab initio* study of the TiO_2-terminated $CaTiO_3$ (001) surface,[5] as well as with other *ab initio* studies dealing with related BO_2-terminated ABO_3 (001) surfaces, such as $PbTiO_3$[32,62] and $BaZrO_3$,[42]

TABLE III: Calculated surface rumpling s, and relative displacements Δd_{ij} between the three near-surface planes, for the CaO- and TiO_2-terminated $CaTiO_3$ (001) surface. Units are percent of the bulk lattice constant.

CaO-terminated			TiO_2-terminated		
s	Δd_{12}	Δd_{23}	s	Δd_{12}	Δd_{23}
7.89	−9.43	1.12	1.61	−4.46	2.75

where the second-layer anion (Pb or Ba) relaxations were larger than the upper-layer (Ti or Zr) ones.

In order to compare the calculated surface structures with experimental results, the surface rumpling s (the relative oxygen displacement relative to the metal atom in the surface layer) and the changes in interlayer distances Δd_{12} and Δd_{23} (where 1, 2 and 3 label the near-surface layers) are presented in Table III. Our calculations of the interlayer distances are based on the positions of the relaxed metal ions (Fig. 1), which are known to be much stronger electron scatters than the oxygen ions.[24] The amplitude of the surface rumpling on the CaO-terminated surface is predicted to be almost five times larger than that for the TiO_2-terminated (001) one. From Table III, one can see that both $CaTiO_3$ (001) surfaces show a reduction of interlayer distance Δd_{12} and an expansion of Δd_{23}. The reduction of interlayer distance Δd_{12} is twice as large for the CaO-terminated surface than it is for the TiO_2-terminated surface. Our calculations dealing with the surface rumpling s, reduction of interlayer distances Δd_{12}, and expansion of interlayer distances Δd_{23} are in qualitative agreement with the only existing *ab initio* study dealing with $CaTiO_3$ (001) surface structures.[5]

To the best of our knowledge there are no experimental measurements with which we can compare our caculated values of s, Δd_{12}, and Δd_{23} on the $CaTiO_3$ (001) surfaces. Even when such data do exist, it is sometimes contradictory, as is the case for the SrO-terminated $SrTiO_3$ (001) surface, where existing LEED[24] and RHEED[25] experiments contradict each other regarding the sign of Δd_{12}.

The calculated atomic displacements, effective static charges, and bond populations between nearest metal and oxygen atoms are given for the TiO_2- and CaO-terminated (001) surfaces in Table IV. The major effect observed here is a strengthening of the Ti-O chemical bond near the surface. Recall from Table I that the Ti and O effective charges ($2.330\,e$ and $-1.371\,e$, respectively) in bulk $CaTiO_3$ are much smaller than expected in an ideal ionic model, and that the Ti-O bond population is $0.084\,e$. Table IV shows that the Ti-O bond population for the TiO_2-terminated (001) surface is considerably larger than the associated bulk value. Comparing with the very small bulk Ca-O bond populations of $0.006\,e$ from Table I, we see that the Ca-O bond populations near the CaO-terminated (001) surface in Table IV are more than three times larger than in the bulk, but more than five times smaller than the Ti-O bond populations on the TiO_2-terminated (001) surface.

TABLE IV: Calculated absolute magnitudes of atomic displacements D (in Å), effective atomic charges Q (in e), and bond populations P (in e) between nearest metal-oxygen pairs, for the for the TiO_2- and CaO-terminated $CaTiO_3$ (001) surfaces.

Layer	Property	Ion	TiO_2-terminated	Ion	CaO-terminated
1	D	Ti	−0.066	Ca	−0.320
	Q		2.278		1.753
	P		0.114		0.020
	D	O	−0.004	O	−0.016
	Q		−1.267		−1.439
	P		0.016		0.070
2	D	Ca	0.106	Ti	0.043
	Q		1.754		2.335
	P		0.006		0.068
	D	O	0.041	O	0.000
	Q		−1.324		−1.425
	P		0.086		0.002
3	D	Ti	—	Ca	—
	Q		2.326		1.786
	P		0.090		0.008
	D	O	—	O	—
	Q		−1.354		−1.381
	P		0.008		0.080

C. $CaTiO_3$ (011) surface structures

As explained in Sec. II, non-polar TiO-, Ca-, and O-terminated surfaces can be constructed for the $CaTiO_3$ (011) surface as in Figs. 3(d)-(f) respectively. Details of the relaxed structures obtained from our calculations for these three terminations are given in Tables V and VI.

On the TiO-terminated (011) surface, the upper-layer Ti atoms move inwards by 7.14% of the bulk lattice constant a_0, whereas the O atoms move outwards by 4.67% (Table V), leading to a large surface rumpling of 11.81% (Table VI), in excellent agreement with the corresponding surface rumpling of 12.10% calculated earlier by Zhang *et al.*[6] The second-layer oxygen atoms move inwards by less than 1% of a_0. The displacement magnitudes of the atoms in the third layer are larger than in the second layer, but smaller than in the top layer. The Δd_{12} values in Table VI show that the reduction of the distance between the first and second layers is three times larger than the corresponding expansion between the second and third layers.

On the Ca-terminated (011) surface, Table V shows that the Ca atoms in the top layer move inwards very strongly, while the O atoms in the second layer only move outwards very weakly. The pattern of oxygen displace-

TABLE V: Calculated atomic relaxations of the $CaTiO_3$ (011) surfaces (in percent of the bulk lattice constant a_0) for the three surface terminations. Positive signs correspond to outward displacements.

Layer	Ion	Δz	Δy
TiO-terminated surface			
1	Ti	−7.14	
1	O	4.67	
2	O	−0.44	
3	Ca	−2.75	
3	O	−3.79	
3	Ti	−0.78	
Ca-terminated surface			
1	Ca	−16.05	
2	O	1.35	
3	Ti	−0.37	
3	O	−1.71	
3	Ca	−0.93	
O-terminated surface			
1	O	−6.10	−2.16
2	Ti	−0.26	−4.70
2	Ca	−2.10	−0.27
2	O	3.43	8.05
3	O	−0.55	1.90

ments is similar to that found on the TiO-terminated (011) surface, in that the inward oxygen displacement in the third layer is larger than the outward displacement in the second layer, but the Ti and Ca displacements in the third layer are smaller than the second-layer oxygen atom displacements.

The O-terminated (011) surface has sufficiently low symmetry that some displacements occur in the y as well as in the z direction. The O atoms in the top layer move mostly inwards (∼6%) but also have some displacement along the surface (∼2%). On the other hand, the second-layer Ti atoms on this surface move strongly along the surface, and also slightly inwards. The second-layer Ca atoms move slightly in the same y direction, and also inwards, while the second-layer O atoms move very strongly in the y direction (but in the opposite direction compared to the top-layer O atoms) and rather strongly outwards. The third-layer O atoms move in the same direction as the second-layer O atoms along the y-axis, but their displacement magnitude are more than four times smaller, and they also move slightly inwards. Table VI shows that there is a substantial contraction of the interlayer distance Δd_{12} and only a very slight expansion of Δd_{23}.

TABLE VI: Surface rumpling s and relative displacements Δd_{ij} (in percent of the bulk lattice constant a_0) for the three near-surface planes on the TiO- and O-terminated $CaTiO_3$ (011) surfaces.

TiO terminated			O terminated	
s	Δd_{12}	Δd_{23}	Δd_{12}	Δd_{23}
11.81	−6.70	2.31	−5.84	0.29

D. $CaTiO_3$ (001) and (011) surface energies

In the present work, we define the unrelaxed surface energy of a given surface termination Λ to be one-half of the energy needed to cleave the crystal rigidly into an unrelaxed surface Λ and an unrelaxed surface with the complementary termination Λ'. For $CaTiO_3$, for example, the unrelaxed surface energies of the complementary CaO- and TiO_2-terminated (001) surfaces are equal, as are those of the TiO- and Ca-terminated (011) surfaces. The relaxed surface energy is defined to be the energy of the unrelaxed surface plus the (negative) surface relaxation energy. These definitions are chosen for consistency with Refs. [12,30]. Unlike the authors of Refs. [29,31,63], we have made no effort to introduce chemical potentials here. Thus, while the values of the surface energies $E_{\rm surf}$ reflect the cleavage energies and thus give some information about trends in the surface energetics, they should be used with caution when addressing questions of the relative stability of surfaces with different stoichiometries in specific environmental conditions.

To calculate the $CaTiO_3$ (001) surface energies, we start with the cleavage energy for the unrelaxed CaO- and TiO_2-terminated surfaces. In our calculations the two 7-layer CaO- and TiO_2-terminated slabs, containing 17 and 18 atoms respectively, represent together 7 bulk unit cells of 5 atoms each. Surfaces with both terminations arise simultaneously under cleavage. According to our definition, we assume that the relevant cleavage energy is distributed equally between created surfaces, so that both the CaO- and TiO_2-terminated surfaces end up with the same unrelaxed surface energy

$$E_{\rm surf}^{\rm (unr)} = \frac{1}{4}[E_{\rm slab}^{\rm (unr)}({\rm CaO}) + E_{\rm slab}^{\rm (unr)}({\rm TiO_2}) - 7E_{\rm bulk}], \quad (1)$$

where $E_{\rm slab}^{\rm (unr)}({\rm CaO})$ and $E_{\rm slab}^{\rm (unr)}({\rm TiO_2})$ are the unrelaxed CaO- and TiO_2-terminated slab energies, $E_{\rm bulk}$ is the energy per bulk unit cell, and the factor of 1/4 comes from the fact that we create four surfaces upon the cleavage procedure. Our calculated unrelaxed surface energy for these surfaces is 1.40 eV, as shown in Table VII. The corresponding relaxation energies are calculated using

$$E_{\rm (rel)}(\Lambda) = \frac{1}{2}[E_{\rm slab}^{\rm (rel)}(\Lambda) - E_{\rm slab}^{\rm (unr)}(\Lambda)], \quad (2)$$

where Λ = CaO or TiO_2 and $E_{\rm slab}^{\rm (rel)}(\Lambda)$ is the slab energy after both sides of the slab have been allowed to relax.

TABLE VII: Calculated cleavage, relaxation, and surface energies for $CaTiO_3$ (001) and (011) surfaces (in eV per surface cell).

Surface	Termination	$E_{surf}^{(unr)}$	E_{rel}	E_{surf}
$CaTiO_3$ (001)	TiO_2	1.40	−0.27	1.13
	CaO	1.40	−0.46	0.94
$CaTiO_3$ (011)	TiO	4.61	−1.48	3.13
	Ca	4.61	−2.70	1.91
	O	3.30	−1.44	1.86

We find relaxation energies of −0.27 and −0.46 eV for the TiO_2-terminated and CaO-terminated surfaces, respectively. The final surface energies are then obtained as a sum of the cleavage and relaxation energies using

$$E_{\rm surf}(\Lambda) = E_{\rm surf}^{\rm (unr)}(\Lambda) + E_{\rm (rel)}(\Lambda). \quad (3)$$

The resulting surface energies of the two (001) surfaces are comparable, but that of the TiO_2-terminated surface is slightly larger than that of the CaO-terminated one (1.13 vs. 0.94 eV), as summarized in Table VII.

In order to calculate the surface energies of the TiO- and Ca-terminated surfaces shown in Fig. 3(d) and (e), containing 16 and 14 atoms respectively, we start with the cleavage energy for unrelaxed surfaces. The two 7-plane Ca- and TiO-terminated slabs represent together six bulk unit cells. The surfaces with both terminations arise simultaneously under cleavage of the crystal, and the relevant cleavage energy is divided equally between these two surfaces, so we obtain cleavage energies according to

$$E_{\rm surf}^{\rm (unr)}(\Lambda) = \frac{1}{4}[E_{\rm slab}^{\rm (unr)}({\rm Ca}) + E_{\rm slab}^{\rm (unr)}({\rm TiO}) - 6E_{\rm bulk}] \quad (4)$$

where Λ denotes Ca or TiO, $E_{\rm slab}^{\rm (unr)}(\Lambda)$ is the energy of the unrelaxed Ca or TiO terminated (011) slab, $E_{\rm bulk}$ is the energy per bulk unit cell, and again the factor of 1/4 arises because four surfaces are created upon cleavage. Our calculated cleavage energy for the Ca or TiO-terminated (011) surfaces of 4.61 eV is more than three times larger than the relevant cleavage energy for the CaO- or TiO_2-terminated (001) surfaces. Finally, the surface energy $E_{\rm surf}(\Lambda)$ is just a sum of the cleavage and relaxation energies, as in Eq. (3).

When we cleave the crystal along (011) in another way, as in Fig. 3(f), we obtain two identical O-terminated surface slabs containing 15 atoms. The cleavage energy of 3.30 eV computed for this O-terminated surface is slightly smaller than for the Ca or TiO-terminated (011) surfaces, but still more than twice as large as for the (001) surfaces. The unit cell of the 7-plane O-terminated slab has the same contents as three bulk unit cells, so the relevant surface energy is just

$$E_{\rm surf}({\rm O}) = \frac{1}{2}[E_{\rm slab}^{\rm (rel)}({\rm O}) - 3E_{\rm bulk}], \quad (5)$$

where $E_{\rm surf}$(O) and $E_{\rm slab}^{\rm (rel)}$(O) are the surface energy and the relaxed slab total energy for the O-terminated (011) surface. The results are again summarized in Table VII. Unlike for the (001) surface, we see that different terminations of the (011) surface lead to large differences in the surface energies. Here the lowest calculated surface energy is 1.86 eV for the O-terminated (011) surface, while the TiO-terminated (3.13 eV) is much more costly than the Ca-terminated (011) surface (1.91 eV).

E. $CaTiO_3$ (011) surface charge distributions and chemical bondings

We present in Table VIII the calculated Mulliken effective charges Q, and their changes ΔQ with respect to the bulk values, for atoms near the surface for the various (011) surface terminations.

On the TiO-terminated surface, the charge on the surface Ti atom is seen to be substantially reduced relative to the bulk, while the metal atoms in the third layer lose much less charge. The O ions in all layers except the central one also have reduced charges, making them less negative. The largest charge change ($0.232\,e$) is observed for subsurface O atoms, giving a large positive change of $0.464\,e$ in the charge for that subsurface layer.

On the Ca-terminated surface, negative changes in the charges are observed for all atoms except for the oxygens in the central layer and the Ti atom in the third layer. The largest charge changes are for the surface Ca ion and the subsurface O ion. The largest overall change in a layer charge ($-0.234\,e$) appears in the subsurface layer as well.

For the O-terminated surface, the negative charge on the surface oxygen is very strongly decreased. Correspondingly, the second layer becomes substantially more negative (overall change $-0.177\,e$), with the change coming mostly on the Ti atom. The total charge density on the third layer is almost unchanged. Negative changes in charge are observed on all central layer atoms, leading to a total charge change of $-0.055\,e$ in that layer.

The interatomic bond populations for the three terminations of the (011) surface are given in Table IX. The major effect observed here is a strong increase of the Ti-O chemical bonding near the TiO- and O-terminated surface as compared to bulk ($0.084\,e$) or to what was found on the TiO_2-terminated (001) surface ($0.114\,e$). For the O-terminated surface, the O(I)-Ti(II) bond population is about twice as large as in the bulk, and about half again as large as at the TiO_2-terminated (001) surface. For the TiO-terminated (011) surface, the Ti-O bond populations are larger in the direction perpendicular to the surface ($0.186\,e$) than in the plane ($0.128\,e$).

TABLE VIII: Calculated Mulliken atomic charges Q, and their changes ΔQ with respect to the bulk, in e, for the three $CaTiO_3$ (011) surface terminations. For reference, the bulk values are 2.330 e (Ti), −1.371 e (O), and 1.782 e (Ca).

Atom (layer)	Q	ΔQ
TiO-terminated surface		
Ti(I)	2.204	−0.126
O(I)	−1.290	0.081
O(II)	−1.139	0.232
Ca(III)	1.733	−0.049
Ti(III)	2.309	−0.021
O(III)	−1.302	0.069
O(IV)	−1.375	−0.004
Ca-terminated surface		
Ca(I)	1.676	−0.106
O(II)	−1.488	−0.117
Ca(III)	1.781	−0.001
Ti(III)	2.334	0.004
O(III)	−1.452	−0.081
O(IV)	−1.363	0.008
O-terminated surface		
O(I)	−1.139	0.232
Ca(II)	1.751	−0.031
Ti(II)	2.235	−0.095
O(II)	−1.422	−0.051
O(III)	−1.359	0.012
Ca(IV)	1.774	−0.008
Ti(IV)	2.310	−0.020
O(IV)	−1.398	−0.027

TABLE IX: The A-B bond populations P (in e) and the relevant interatomic distances R (in Å) for three different (011) terminations of the $CaTiO_3$ surface. Symbols I-IV denote the number of each plane enumerated from the surface. The nearest neighbor Ti-O distance in the unrelaxed bulk is 1.926 Å.

Atom A	Atom B	P	R
TiO-terminated surface			
Ti(I)	O(I)	0.128	1.979
	O(II)	0.186	1.752
O(II)	Ti(III)	0.110	1.935
	Ca(III)	0.018	2.769
	O(III)	−0.024	2.790
Ti(III)	Ca(III)	0.000	3.336
	O(III)	0.100	1.929
	O(IV)	0.076	1.904
Ca(III)	O(III)	0.008	2.723
	O(IV)	0.004	2.672
O(III)	O(IV)	−0.032	2.653
Ca-terminated surface			
Ca(I)	O(II)	0.006	2.458
O(II)	Ca(III)	0.012	2.768
	Ti(III)	0.072	1.973
	O(III)	−0.036	2.784
Ca(III)	O(III)	0.002	2.723
	O(IV)	0.006	2.705
Ti(III)	O(III)	0.060	1.926
	Ca(III)	0.000	3.335
	O(IV)	0.084	1.915
O(III)	O(IV)	−0.064	2.691
O-terminated surface			
O(I)	Ca(II)	0.028	2.613
	Ti(II)	0.162	1.699
	O(II)	−0.016	2.788
Ca(II)	O(II)	−0.006	2.412
	Ti(II)	0.002	3.198
Ti(II)	O(II)	0.086	1.992
	O(III)	0.100	1.764
O(II)	O(III)	0.010	2.925
Ca(II)	O(III)	0.006	2.737
O(III)	O(IV)	−0.038	2.750
	Ti(IV)	0.062	1.963
	Ca(IV)	0.004	2.677

IV. CONCLUSIONS

According to the results of our *ab initio* hybrid B3PW calculations, all of the upper-layer atoms for the TiO_2- and CaO-terminated $CaTiO_3$ (001) surfaces relax inwards, while outward relaxations of all atoms in the second layer are found at both kinds of (001) terminations. These results are typical for other technologically important ABO_3 perovskites such as $BaTiO_3$, $PbTiO_3$, and $BaZrO_3$.[32,42,61,62] However, they contrast with the only previous *ab initio* study of $CaTiO_3$ (001) surfaces by Wang *et al.*,[5] where the authors found that the first-layer O atoms relax outwards on the CaO-terminated (001) surface. For the TiO_2-terminated (001) surface, our largest relaxation is on the second-layer atoms, not on the first-layer ones, this time in agreement with Wang *et al.*[5] The stronger relaxation of the second-layer atoms compared to the first-layer ones was found by us earlier also for TiO_2-terminated $PbTiO_3$ and $SrTiO_3$ (001) surfaces.[7,32] Our calculations of the CaO-terminated (001) surface shows a very strong inward relaxation of 8.31% for the top-layer Ca atoms, in very good quantitative agreement with the inward relaxation of 8.80% found by Wang *et al.*[5] This inward relaxation of the surface Ca atoms on the CaO-terminated (001) surface is much stronger than was obtained for the AO-terminated (001) surfaces of other ABO_3 perovskites (A = Sr, Ba, Pb, and Zr).[7,32,42,61,62]

Our calculated surface rumpling of 7.89% for the CaO-terminated (001) surface is almost five times larger than that of the corresponding TiO_2-terminated surface, and is comparable with the surface rumpling of

9.54% obtained for the CaO-terminated surface by Wang *et al.*[5] This rumpling is larger than the rumplings obtained in previous *ab initio* calculations for the AO-terminated (001) surfaces of $SrTiO_3$, $BaTiO_3$, $BaZrO_3$, and $PbTiO_3$.[7,20,21,32,42,61,62]

Our calculations predict a compression of the interlayer distance between first and second planes, and an expansion between second and third planes, for the (001) surfaces. Our value for Δd_{12} of -9.43% on the CaO-terminated (001) surface is in a reasonable agreement with the result of -11.43% obtained by Wang *et a.*[5] and is larger than the corresponding value for $_3$, $BaTiO_3$, $BaZrO_3$, and $PbTiO_3$ (001) surfaces.[7,20,21,32,42,61,62] As for experimental confirmation of these results, we are unfortunately unaware of experimental measurements of Δd_{12} and Δd_{23} for the $CaTiO_3$ (001) surfaces. Moreover, for the case of the SrO-terminated $SrTiO_3$ (001) surface, existing LEED[24] and RHEED[25] experiments actually contradict each other regarding the sign of Δd_{12}. In view of the absence of clear experimental determinations of these parameters, therefore, the first-principles calculations are a particularly important tool for understanding the surface properties.

Turning now to the $CaTiO_3$ (011) surfaces, we found that the inward relaxation of the upper-layer metal atom on the TiO-terminated (011) surface (Ti displacement of 7.14%) is smaller than on the CaO-terminated (001) surface (Ca displacement of 8.31%), in contrast to what was found for the $SrTiO_3$, $BaTiO_3$, $PbTiO_3$, and $BaZrO_3$ surfaces.[7,20,21,32,42,61,62] However, the inward relaxation by 16.05% of the upper-layer Ca atom on the Ca-terminated (011) surface is about twice as large as the inward relaxations of surface atoms obtained on the CaO-terminated (001) surface. Our calculated atomic displacements in the third plane from the surface for the Ca, TiO, and O-terminated (011) surfaces are still substantial. Our calculated surface rumpling s for the TiO-terminated (011) surface is approximately 1.5 times larger than that of the CaO-terminated (001) surface, and many times times larger than that of the TiO_2-terminated (001) surface. Also, our *ab initio* calculations predict a compression of the interlayer distance Δd_{12} and an expansion of Δd_{23} for the TiO- and O-terminated (011) surfaces. This behavior seems to be obeyed by all previous calculations of relaxations at (001) ABO_3 perovskite surfaces[7,20,21,32,61,62]; we can conclude that this effect may be a general rule, requiring further experimental studies and confirmation.

A comparison of our *ab initio* B3PW calculations on the TiO-terminated $CaTiO_3$ (011) surface with the previous *ab initio* calculation performed by Zhang et al.[6] shows that the atomic displacement directions almost always coincide, the only exception being the small third-layer Ti-atom inward relaxation of -0.78% in our calculation compared with an outward one of 0.28% in theirs. The displacement magnitudes are generally comparable in the two studies, leading to an excellent agreement for the TiO-terminated (011) surface rumplings (11.81% in our calculations vs. 12.10% in theirs). For the Ca-terminated (011) surface, our inward relaxation magnitude of 16.05% for the upper-layer Ca atom, the largest of all atoms on all of the studied (011) terminations, is in excellent agreement with the value of 15.37% obtained in Ref. [6]. This largest displacement of the surface A atom on the A-terminated (011) surface is was also obtained for the $SrTiO_3$, $BaTiO_3$, $PbTiO_3$, and $BaZrO_3$ cases.[7,20,21,32,42,61,62] Just as they did for the TiO-terminated (011) surface, our relaxation directions for the Ca-terminated surface almost all coincide with those obtained previously,[6] the only exception being again the displacement direction of the third-layer Ti atom. We find that this atom moves slightly inwards by 0.37%, whereas the previous work obtain an outward relaxation of 0.89%.[6]

For the O-terminated (011) surface, in most cases our calculated displacement directions are in qualitative agreement with the results of Ref. [6]. In some cases, as for example for the second layer Ti and O atom displacements in the direction along the surface, our calculated displacement magnitudes for Ti (4.70%) and for O (8.05%) are in an excellent agreement with the corresponding results (4.53% and 8.06% respectively) of Zhang *et al.*[6] However, in many cases, our calculated displacement magnitude is smaller than that calculated in Ref. [6]. Most disturbingly, in three cases there are also some qualitative differences between our results and those of Zhang *et al.*[6] Specifically, the second-layer Ca and Ti atoms move substantially inwards in our calculations, but outwards in Ref. [6], and the third-layer O atoms move in opposite directions in the two calculations.

As for the surface energies, we find that both the CaO- and TiO_2-terminated (001) surfaces are about equally favorable, with surface energies of 0.94 and 1.13 eV respectively. These values are in excellent agreement with the corresponding values of 0.824 and 1.021 eV respectively as computed by Zhang *et al.* in Ref. [6]. In contrast, we see very large differences in surface energies on the (011) surfaces. Our lowest-energy (011) surface is the O-terminated one at 1.86 eV, with the Ca-terminated surface just behind at 1.91 eV, and the TiO-terminated surface is very unfavorable at 3.13 eV. These are all much larger, by about a factor of two or more, than for the (001) surfaces. This is the same ordering of (011) surface energies as was obtained by Zhang *et al.*, but these authors obtained quite different values of 0.837, 1.671, and 2.180 eV for the O-, Ca-, and TiO-terminated (011) surfaces, respectively.[6] The values for the Ca- and TiO-terminated surface energies are only modestly smaller than ours, but the value for the O-terminated (011) surface energy presents a clear disagreement with the present work, being more than twice as small as ours. In fact, according to their work, the O-terminated (011) surface is even lower in energy than the TiO_2-terminated (001) surface, and about equal to that of the CaO-terminated (001) surface. In this respect, their result contrasts not only with our result for

$CaTiO_3$, but with all previous *ab initio* and shell-model calculations dealing with $SrTiO_3$, $BaTiO_3$, $PbTiO_3$, and $BaZrO_3$ (001) and (011) surface energies,[7,12,21,23,30,32,42] where the (001) surface energies are always smaller than the (011) surface energies.

We do not understand the reason for this discrepancy. We have carried out test calculations of the cleavage energies of the three (011) surfaces using the PBE-GGA exchange-correlation functional[64] used by Zhang *et al.*, but within the CRYSTAL-2003 code package, and we find cleavage energies that are only about 15-25% larger than theirs. The drastic difference, then, must be in the relaxation energy of the Ca-terminated surface, which is $-1.83\,\mathrm{eV}$ in our calculation and $-2.70\,\mathrm{eV}$ in theirs. We also did a test calculation of the energy of a Ca-terminated (011) slab in which the surface atoms were placed by hand at the coordinates reported for this surface in Ref. [6], and found that the energy was even higher than the energy of the unrelaxed structure. Clearly these discrepancies call for further exploration.

Our *ab initio* calculations indicate a considerable increase in the Ti-O bond covalency near the TiO- and O-terminated (011) surfaces, as well as the TiO_2-terminated (001) surface. The Ti-O bond covalency at the TiO-terminated (011) surface ($0.128\,e$) is much larger than that for the TiO_2-terminated (001) surface ($0.114\,e$) or in bulk $CaTiO_3$ ($0.084\,e$). The Ti-O bond populations on the TiO-terminated (011) surface are much larger in the direction perpendicular to the surface than in the plane (0.186 vs. $0.128\,e$). Our calculated increase of the Ti-O bond covalency near the (011) surface, is in agreement with the resonant photoemission experiments.[65] This should have an impact on the electronic structure of surface defects (e.g., F centers),[66] as well as on the adsorption and surface diffusion of atoms and small molecules relevant for catalysis.

V. ACKNOWLEDGMENTS

The present work was supported by Deutsche Forschungsgemeinschaft (DFG) and by ONR Grant No. N00014-05-1-0054.

[1] J. F. Scott, *Ferroelectric Memories* (Springer, Berlin, 2000).
[2] M. Dawber, K. M. Rabe, and J. F. Scott, Rev. Mod. Phys. **77**, 1083 (2005).
[3] R. E. Cohen, Nature, **358**, 136 (1992).
[4] A. E. Ring, S. E. Kesson, K. D. Reeve, D. M. Levins, E. J. Ramm, in: W. Lutze, R. C. Ewings (Eds.), *Radioactive Waste Forms for the Further*, (North Holland Publishing, Amsterdam, 1987).
[5] Y. X. Wang, M. Arai, T. Sasaki, and C. L. Wang, Phys. Rev. B **73**, 035411 (2006).
[6] J. M. Zhang, J. Cui, K. W. hu, V. Ji, Z. Y. Man, Phys. Rev. B **76**, 115426 (2007).
[7] R. I. Eglitis, and D. Vanderbilt, Phys. Rev. B **77**, 195408 (2008).
[8] S. Kimura, J. Yamauchi and M. Tsukada, Phys. Rev. B **51**, 11049 (1995).
[9] Z. Q. Li, J. L. Zhu, C. Q. Wu, Z. Tang and Y. Kawazoe, Phys. Rev. B **58**, 8075 (1998).
[10] R. Herger, P. R. Willmott, O. Bunk, C. M. Schlepütz, B. D. Patterson and B. Delley, Phys. Rev. Lett. **98**, 076102 (2007).
[11] N. Erdman, K. Poeppelmeier, M. Asta, O. Warschkow, D. E. Ellis and L. Marks, Nature **419**, 55 (2002).
[12] E. Heifets, R. I. Eglitis, E. A. Kotomin, J. Maier, and G. Borstel, Phys. Rev. B **64**, 235417 (2001).
[13] E. Heifets, R. I. Eglitis, E. A. Kotomin, J. Maier, and G. Borstel, Surf. Sci. **513**, 211 (2002).
[14] K. Johnston, M. R. Castell, A. T. Paxton and M. W. Finnis, Phys. Rev. B **70**, 085415 (2004).
[15] R. I. Eglitis, S. Piskunov, E. Heifets, E. A. Kotomin, and G. Borstel, Ceram. Int. **30**, 1989 (2004).
[16] S. Piskunov, E. A. Kotomin, E. Heifets, J. Maier, R. I. Eglitis and G. Borstel, Surf. Sci. **575**, 75 (2005).
[17] R. Herger, P. R. Willmot, O. Bunk, C. M. Schlepütz, B. D. Patterson, S. Delley, V. L. Schneerson, P. F. Lyman, and D. K. Saldin, Phys. Rev. B **76**, 195435 (2007).
[18] C. H. Lanier, A. van de Walle, N. Erdman, E. Landree, O. Warschkow, A. Kazimirov, K. R. Poeppelmeier, J. Zegenhagen, M. Asta and L. D. Marks, Phys. Rev. B **76**, 045421 (2007).
[19] Y. L. Li, S. Choudhury, J. H. Haeni, M. D. Biegalski, A. Vaudevarao, A. Sharan, H. Z. Ma, J. Levy, V. Gopalan, S. Trolier-McKinstry, D. G. Schlom, Q. X. Jia and L. Q. Chen, Phys. Rev. B **73**, 184112 (2006).
[20] C. Cheng, K. Kunc, M. H. Lee, Phys. Rev. B **62**, 10409 (2000).
[21] J. Padilla and D. Vanderbilt, Surf. Sci. **418**, 64 (1998).
[22] V. Ravikumar, D. Wolf and V. P. Dravid, Phys. Rev. Lett. **74**, 960 (1995).
[23] E. Heifets, E. A. Kotomin, and J. Maier, Surf. Sci. **462**, 19 (2000).
[24] N. Bickel, G. Schmidt, K. Heinz, and K. Müller, Phys. Rev. Lett. **62**, 2009 (1989).
[25] T. Hikita, T. Hanada, M. Kudo, and M. Kawai, Surf. Sci. **287-288**, 377 (1993).
[26] M. Kudo, T. Hikita, T. Hanada, R. Sekine, and M. Kawai, Surf. Interface Anal. **22**, 412 (1994).
[27] Y. Kido, T. Nishimura, Y. Hoshido, and H. Mamba, Nucl. Instrum. Methods Phys. Res. B **161-163**, 371 (2000).
[28] G. Charlton, S. Brennan, C. A. Muryn, R. McGrath, D. Norman, T. S. Turner, and G. Thorton, Surf. Sci. **457**, L376 (2000).
[29] F. Bottin, F. Finocchi, and C. Noguera, Phys. Rev. B **68**, 035418 (2003).
[30] E. Heifets, W. A. Goddard III, E. A. Kotomin, R. I. Eglitis, and G. Borstel, Phys. Rev. B **69**, 035408 (2004).
[31] E. Heifets, J. Ho, and B. Merinov, Phys. Rev. B **75**, 155431 (2007).
[32] R. I. Eglitis, and D. Vanderbilt, Phys. Rev. B **76**, 155439

(2007).
[33] H. Bando, Y. Aiura, Y. Haruyama, T. Shimizu, Y. Nishihara, J. Vac. Sci. Technol. B **13**, 1150 (1995).
[34] K. Szot, and W. Speier, Phys. Rev. B **60**, 5909 (1999).
[35] J. Brunen, J. Zegenhagen, Surf. Sci. **389**, 349 (1997).
[36] Q. D. Jiang, J. Zegenhagen, Surf. Sci. **425**, 343 (1999).
[37] J. Zegenhagen, T. Haage, Q. D. Jiang, Appl. Phys. A **67**, 711 (1998).
[38] R. Souda, Phys. Rev. B **60**, 6068 (1999).
[39] Y. Adachi, S. Kohiki, K. Wagatsuma, M. Oku, J. Appl. Phys. **84**, 2123 (1998).
[40] A. D. Becke, J. Chem. Phys. **98**, 5648 (1993).
[41] J. P. Perdew, and Y. Wang, Phys. Rev. B **33**, 8800 (1986); J. P. Perdew, and Y. Wang, *ibid.*, **40**, 3399(E) (1989); J. P. Perdew, and Y. Wang, *ibid.*, **45**, 13244 (1992).
[42] R. I. Eglitis, J. Phys.: Condens. Matter **19**, 356004 (2007).
[43] V. R. Saunders, R. Dovesi, C. Roetti, M. Causa, N. M. Harrison, R. Orlando, C. M. Zicovich-Wilson, *CRYSTAL-2003 User Manual*, University of Torino, Torino, Italy, 2003.
[44] S. Piskunov, E. Heifets, R. I. Eglitis, and G. Borstel, Comput. Mater. Sci. **29**, 165 (2004).
[45] H. Shi, R. I. Eglitis, and G. Borstel, Phys. Rev. B **72**, 045109 (2005).
[46] P. J. Hay, and W. R. Wadt, J. Chem. Phys. **82**, 270 (1985); P. J. Hay, and W. R. Wadt, *ibid.* **82**, 284 (1985); P. J. Hay, and W. R. Wadt, *ibid.* **82**, 299 (1985).
[47] H. J. Monkhorst, and J. D. Pack, Phys. Rev. B **13**, 5188 (1976).
[48] C. Noguera, J. Phys.: Condens. Matter **12**, R367 (2000).
[49] P. W. Tasker, J. Phys. C: Solid State Phys. **12**, 4977 (1979).
[50] A. Pojani, F. Finocchi, and C. Noguera, Surf. Sci. **442**, 179 (1999).
[51] A. Granicher and O. Jakits, Nuove Cimento Suppl. **9**, 480 (1954).
[52] H. F. Kay and P. C. Bailey, Acta Crystallogr. **10**, 437 (1957).
[53] X. Liu and R. C. Liebermann, Phys. Chem. Minerals **20**, 171 (1993).
[54] B. J. Kennedy, C. J. Howard, and B. C. Chakoumakos, J. Phys. Cond. Matt. **11**, 1479 (1999).
[55] A. M. Glazer, Acta Crystallogr., Sect. B: Struct. Crystallogr. Cryst. Chem. **28**, 3384 (1972).
[56] D. Vanderbilt and W. Zhong, Ferroelectrics **206-207**, 181 (1998).
[57] E. Cockayne and B. P. Burton, Phys. Rev. B **62**, 3735 (2000).
[58] *Ferroelectrics and Related Substances*, edited by K. H. Hellwege, and A. M. Hellwege, Landolt-Bornstein, New Series, Group III, Vol. **3** (Springer Verlag, Berlin, 1969).
[59] C. R. A. Catlow, and A. M. Stoneham, J. Phys. C: Solid State Phys. **16**, 4321 (1983).
[60] R. C. Bochiccio, and H. F. Reale, J. Phys. B: At. Mol. Opt. Phys. **26**, 4871 (1993).
[61] J. Padilla, and D. Vanderbilt, Phys. Rev. B **56**, 1625 (1997).
[62] B. Meyer, J. Padilla, and D. Vanderbilt, Faraday Discuss. **114**, 395 (1999).
[63] K. Rapcewics, B. Chen, B. Yakobsen, J. Bernhok, Phys. Rev. B **57**, 7281 (1998).
[64] J. P. Perdew, K. Burke, and M. Ernzerhof, Phys. Rev. Lett. **77**, 3865 (1996).
[65] R. Courths, B. Cord, H. Saalfeld, Solid State Commun. **70**, 1047 (1989).
[66] R. I. Eglitis, N. E. Christensen, E. A. Kotomin, A. V. Postnikov, and G. Borstel, Phys. Rev. B **56**, 8599 (1997).